

PRECURSORS OF UCHII REGIONS & THE EVOLUTION OF MASSIVE OUTFLOWS

Henrik Beuther

*Harvard-Smithsonian Center for Astrophysics
60 Garden Street
Cambridge, MA 02138
USA*

hbeuther@cfa.harvard.edu

Debra Shepherd

*National Radio Astronomy Observatory
Socorro, NM 87801
USA*

dshepher@nrao.edu

Abstract

Since this contributions was meant to cover two subjects which are both in the field of massive star formation but which in its details can be discussed separately, this paper is divided in two sections. First, we present characteristics of precursors of UCHII regions and their likely evolutionary properties. The second section discusses massive molecular outflows, their implications for high-mass star formation, and a possible evolutionary sequence for massive outflows.

Keywords: stars: early type; stars: formation; ISM: jets and outflows; ISM: molecules

1. Precursors of UCHII regions

Evolutionary scenarios suggest that High-Mass Starless Cores (HMSCs) represent the earliest evolutionary stage of massive star formation (e.g., Evans et al., 2002). The next observable evolutionary stage is when a High-Mass Protostellar Object (HMPO) forms in the core producing strong millimeter continuum and mid-infrared emission but no detectable centimeter continuum due to free-free emission from ionized gas (e.g., Molinari et al., 1996, Sridharan et al., 2002). The lack of detectable free-free emission may be because the protostar has not reached the main sequence or because the accretion rate onto the stellar surface is high enough to quench a developing HII region (e.g., Walmsley, 1995, Churchwell, 2002). Hot Cores are considered to belong to the HMPO stage. Soon after the hot core is formed, the central massive protostar produces adequate ionizing radiation to form a hypercompact, unresolved, most likely optically thick HII region (HCHII). The HCHII region may still be partially quenched by infalling gas which can hinder the expansion of the hypercompact HII region (e.g., Walmsley, 1995, Keto, 2003). Eventually, the hypercompact HII region begins to expand forming the well-studied ultracompact HII region

(e.g., Wood and Churchwell, 1989, Kurtz et al., 1994) and later a more evolved HII region. Theoretical model calculations estimate an evolutionary time-scale for massive star formation of about 10^5 yrs, assuming that massive stars form via accretion-based processes similar to low-mass star formation (McKee and Tan, 2002). A key difference between low- and high-mass star formation is that massive stars reach the main sequence while still actively accreting; low-mass stars end their accretion phase before they reach the main sequence. Here, we discuss the properties of the precursors of ultracompact HII regions, namely HMPOs and HMSCs.

1.1 High-Mass Protostellar Objects (HMPOs)

There are several review articles that discuss the earliest stages of massive star formation and cover different aspects of the topic in more depth than possible here (e.g., Garay and Lizano, 1999, Kylafis and Pavlakis, 1999, Kurtz et al., 2000, Churchwell, 2002, Cesaroni, 2004). Therefore, we focus on the basic characteristics of HMPOs and discuss a few recent results in this field.

Basic characteristics. The far-infrared colors of HMPOs are similar to those of UCHII regions (e.g., Wood and Churchwell, 1989, Sridharan et al., 2002). This is mainly due to the fact that they resemble each other with regard to their gas/dust temperatures and the presence of dense gas. A major observational difference is that HMPOs show no or only weak cm continuum emission, thus the central objects have not yet produced a significant ionized region to trigger the necessary free-free emission. While most of the UCHII region luminosity is due to a central H-burning star, a large fraction of the HMPO luminosity is still expected to be due to accretion (e.g., Sridharan et al., 2002). Furthermore, the average observed $\text{NH}_3(1,1)$ linewidth toward HMPOs is $\Delta v \sim 2.1$ km/s compared to average values toward UCHII regions of $\Delta v \sim 3.1$ (Sridharan et al., 2002). This difference implies less turbulent motions at the HMPO stage.

Furthermore, often H_2O and/or Class II CH_3OH maser emission is observed toward HMPOs (e.g., Walsh et al., 1998, Beuther et al., 2002d, Codella et al., 2004). The existence of one or the other type of maser emission is widely regarded as a good signpost for massive star formation (in spite of H_2O maser emission being also observed toward low-mass star-forming regions), but nevertheless, there is no general agreement about the physical processes generating the maser emission. There is indicative evidence that both maser types are produced either within accretion disks or molecular outflows (e.g., Norris et al., 1998, Walsh et al., 1998, Torrelles et al., 1998, Minier et al., 2000, Codella et al., 2004). Although H_2O and Class II CH_3OH masers are produced during the early stages of massive star formation, it appears that in general they cannot be used to derive the underlying physical processes of the regions. This state-

ment does not exclude the possibility that in selected sources very high-spatial resolution and proper motion studies of masers can constrain the processes triggering the maser emission (for prominent recent examples see, e.g., Torrelles et al., 2003, Pestalozzi et al., 2004).

Millimeter continuum emission. Observations of HMPOs in (sub)mm continuum emission have shown that they exhibit strong dust continuum emission from massive dust and gas cores (e.g., Molinari et al., 2000, Beuther et al., 2002b, Mueller et al., 2002, Williams et al., 2004). Even with the rather coarse spatial resolution of most single-dish investigations ($\geq 11''$ beam), the gas cores often show filamentary and multiple structures. The density distribution of the cores are usually well fitted by power-law distributions and the power-law indices are in most cases around 1.6 (e.g., Beuther et al., 2002b, Mueller et al., 2002), similar to the power-law indices of young low-mass cores (e.g., Motte et al., 1998). Furthermore, multi-wavelength investigations show that the dust opacity index β toward HMPOs is significantly lower than toward UCHII regions (mean values of 0.9 versus 2.0, Williams et al., 2004, Hunter, 1997). In low-mass cores, low dust opacity indices are attributed either to increasing opacity or grain growth at early evolutionary stages (e.g., Hogerheijde and Sandell, 2000, Beckwith et al., 2000). In contrast, Williams et al. (2004) show for their sample that the lowest observed values for β are associated with lower rather than higher opacities. Thus, these observations are consistent with grain growth in the early evolutionary stages of the dense cores. However, a point of caution remains because significant grain growth is expected to take at least 10^5 years (e.g., Ossenkopf and Henning, 1994) whereas the whole massive star formation process might only last for $\sim 10^5$ years (McKee and Tan, 2002). If these time-scales are correct it may be difficult to produce similarly large grains in high-mass cores compared to their low-mass counterparts and the observed low values of β might require a different interpretation.

Fragmentation and the Initial Mass Function (IMF). One important question for the whole cluster formation process is: At what evolutionary stage does the Initial Mass Function gets established? Do the initial fragmentation processes of the massive cores already show signatures of the IMF, or is competitive accretion during the ongoing cluster formation the main driver of the IMF (e.g., Bonnell et al., 2004)? Within the last two years, there have been published a few very different studies which investigate the protocluster mass distribution and its connection to the IMF: Shirley et al., 2003, analyze single-dish CS observations toward a sample of 63 massive H₂O maser sources with $\sim 30''$ resolution, Williams et al., 2004, do a similar study based on single-dish (sub)mm continuum observations with $8'' - 15''$ resolution, and Beuther and Schilke, 2004, observe one HMPO in the mm continuum emission at $1.5'' \times 1''$

Figure 1. Compilation of mass distributions from very young high-mass star-forming regions: the cumulative mass distribution to the left is from single-dish CS observations of a sample of massive H₂O maser sources (Shirley et al., 2003, LS and RE correspond to Least Square and Robust estimation fits). The cumulative mass spectrum in the middle is from single-dish mm dust continuum observations of a sample of HMPOs (Williams et al., 2004, the dotted and full lines correspond to far and near kinematic distances, respectively). The protocluster mass function to the right is from high-spatial resolution PdBI observations of one HMPO IRAS 19410+2336 (Beuther and Schilke, 2004, the full line is the best fit to the data, and the dashed and dotted lines present the IMFs derived from Salpeter, 1955, and Scalo, 1998).

resolution with the Plateau de Bure Interferometer. The main difference between the two single-dish studies and the interferometric investigation is that the single-dish observations average out whole young clusters and thus need many clusters to derive a cumulative mass distribution of the sample of protoclusters, whereas Beuther & Schilke (2004) only investigate one young cluster but are capable of resolving many sources within this cluster. All of the above mentioned studies preferentially select regions that are in the earliest evolutionary stages of star formation and most have not yet formed detectable UCHII regions. Figure 1 summarizes the results from the three studies.

Since the observations and the analysis are very different, the completeness limits of the Shirley et al. and Williams et al. studies are different as well (> 1000 and $> 10 M_{\odot}$, respectively). Nevertheless, both studies find above their completeness limits power-law distributions comparable to the IMF. Similarly but on much smaller spatial scales, Beuther & Schilke (2004) also find a good correspondence between the protocluster mass spectrum in IRAS 19410+2336 compared with the IMFs as derived by, e.g., Salpeter, 1955, Scalo, 1998. These independently derived results are encouraging support for the idea that the early fragmentation of massive star-forming cores is responsible for the determination of the IMF, and not processes which might take place at evolutionary later stages like competitive accretion. An additional result from the single-dish observations alone is that the star-formation efficiency for the sample of protoclusters is relatively mass invariant (Williams et al., 2004).

Chemistry. Young massive star-forming regions and especially Hot Cores are known to have an incredibly rich chemistry (e.g., the rich spectra toward the Orion-KL Hot Core, e.g., Blake et al., 1987, Schilke et al., 1997). Here, we present recent submillimeter observations of the prototypical Hot Core Orion-KL. A more detailed discussion of core chemistry is presented in Paola Caselli's contribution to this volume.

Beuther et al., 2004b, used the Submillimeter Array (SMA) to image the submm line and continuum emission of Orion-KL at sub-arcsecond resolution. In the submm continuum, the enigmatic source "T" could be disentangled from the Hot Core, and source "n" was detected for the first time shortward of 7 mm (Beuther et al., 2004b). Additionally, within one spectral setup of the SMA

(4 GHz combining the upper and lower sideband) approximately 150 molecular lines were observed (Beuther et al. in prep.). Figure 2 shows example line images which highlight the spatial variations observed between the different molecular species: SiO is detected mainly from the outflow emanating from source “I”, but all other molecules peak offset from source “I”. Typical hot

Figure 2. Submm line images obtained with the SMA at 865 μm (Beuther et al. in prep.). The grey-scale and contours show the molecular emission as labeled at the bottom left of each panel. The three stars mark the positions of source “I”, the Hot Core mm continuum peak, and source “n” (labeled at the bottom-right).

core molecules like CH_3CN or $\text{CH}_3\text{CH}_2\text{CN}$ show the hot core morphology previously reported from, e.g., NH_3 observations (Wilson et al., 2000). Contrary to this, CH_3OH does show some hot core emission as well, but there is an additional strong CH_3OH peak further south associated with the so called compact ridge emission. Other molecules like C^{34}S or $\text{C}_2\text{H}_5\text{OH}$ show even different spatial emission, tracing partly the hot core and the compact ridge but also showing an additional peak to the north-west that is spatially associated with IRC6. We still do not properly understand the underlying reasons for this spatial molecular diversity, but these observations of the closest Hot Core, Orion-KL, stress that we must be cautious in our interpretations of spatial structures for other Hot Cores that are typically at much greater distances.

1.2 High-Mass Starless Cores (HMSCs)

Prior to the infrared satellites ISO and MSX, there was no observational evidence for High-Mass Starless Cores, and HMPOs were considered to be the youngest observationally accessible stage of massive star formation. The detection of Infrared Dark clouds (IRdCs) and their association with mm dust continuum emission changed that situation (e.g., Egan et al., 1998), and since then observational studies of these HMSCs/IRdCs have begun to shed first light on this evolutionary stage. Evans et al., 2002, outlined potential properties of HMSC, and recently Garay et al., 2004, presented an analysis of four such sources. Here, we present an approach to identify and study HMSCs based on a comparison of previously derived mm continuum maps of HMPOs (Beuther et al., 2002b) with the MSX database (Sridharan et al. in prep.).

Based on an initial study of HMPOs associated with IRAS sources (Sridharan et al., 2002), Beuther et al., 2002b, observed serendipitously within the same fields of view a number of secondary mm-peaks which were not associated with IRAS sources. Correlation of these mm-peaks with the MSX mid-infrared observations revealed a number of mm-peaks which are not only

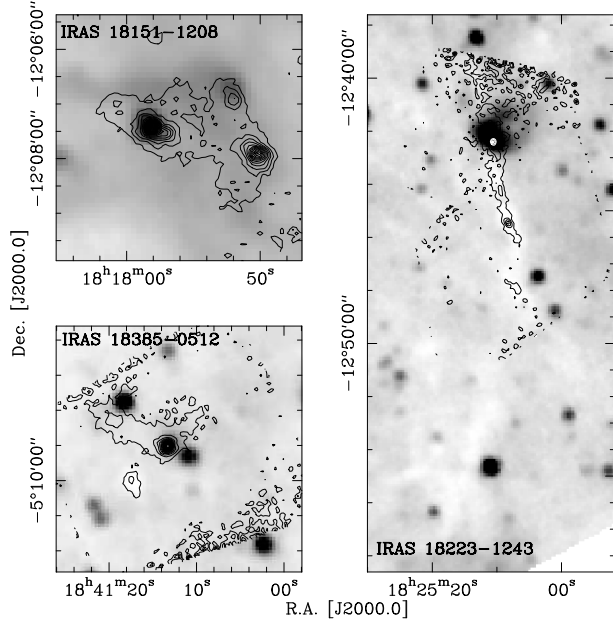


Figure 3. The grey-scale shows the $8\text{ }\mu\text{m}$ emission from the MSX satellite, and the contours present the 1.2 mm continuum emission first presented in Beuther et al., 2002b.

weak in the mid-infrared but which are seen as absorption shadows against the galactic background (Fig. 3, Sridharan et al. in prep.).

Observing these HMSCs with the Effelsberg 100 m telescope in NH_3 (Sridharan et al. in prep.), the derived average temperatures are around 15 K compared to the average temperatures of the more evolved HMPOs of 22 K. Furthermore, we find on average a smaller linewidth of 1.6 km/s toward the HMSCs in comparison to a mean value of 2.1 km/s observed toward the HMPOs. With gas masses of the order a few hundred M_\odot , no mid-infrared emission, cold temperatures and less turbulence implied by the small line-widths, these sources are promising candidates for being HMSCs on the verge of forming massive clusters. Ongoing single-dish and interferometric follow-up observations of this and other samples will hopefully improve our understanding of the initial conditions of massive star formation significantly.

2. Massive molecular outflows: an evolutionary scenario

In contrast to low-mass outflows, there is no general census for the understanding of massive molecular outflows. For recent reviews on different aspects of massive molecular outflows see Bachiller and Tafalla, 1999, Church-

well, 1999, Richer et al., 2000, Shu et al., 2000, Konigl and Pudritz, 2000, Shepherd, 2003, Beuther, 2004.

Two competing scenarios have been put forth to explain the formation of massive stars: one possibility is to extend the low-mass models to high-mass star formation and form massive stars via enhanced accretion processes through accretion disks (e.g., Jijina and Adams, 1996, Norberg and Maeder, 2000, Yorke and Sonnhalter, 2002, McKee and Tan, 2003). Contrary to this, at the dense centers of evolving massive clusters, competitive accretion could become dominant and it might even be possible that (proto)stellar mergers occur and form the most massive objects via coagulation processes (e.g., Bonnell et al., 1998, Stahler et al., 2000, Bally, 2002, Bonnell et al., 2004). Massive molecular outflows can help to differentiate between these scenarios: while the enhanced accretion model predicts collimated molecular outflows with properties similar to those for low-mass outflows, it is unlikely that highly-collimated structures could exist in the coalescence scenario and the outflow energetics would be significantly different.

2.1 Summary of observational constraints

Observations of massive molecular outflows are unfortunately not conclusive. On the one hand, some observations find that molecular outflows from high-mass star-forming regions appear less collimated than outflows from low-mass regions (e.g., Shepherd and Churchwell, 1996a, Ridge and Moore, 2001, Wu et al., 2004). However, it has been shown that the lower collimation factors of massive outflows observed with single-dish telescopes could simply be due to the on average larger distances of high-mass star-forming regions (Beuther et al., 2002c). A few interferometric observations with $0.1'' - 10''$ resolution suggest that outflow opening angles from at least some young, early-B stars can be significantly wider than those seen toward low-mass protostars (e.g., Shepherd et al., 1998, Shepherd et al., 2001, Shepherd et al., 2003). Thus, greater distances and the associated lower angular resolution is not the only reason for the observed poor collimation in some massive outflows. There is also evidence that the energetics in at least one massive outflow from an early B star in W75N are different to those in low-mass outflows, although exactly what this implies is unclear (Shepherd et al., 2003).

In recent years a few examples of collimated massive outflows from early B stars have been found (e.g., Beuther et al., 2002a, Gibb et al., 2003, Su et al., 2004). A comparison of position-velocity diagrams from collimated massive molecular outflows with their low-mass counterparts reveal similar signatures from outflows of all masses (Beuther et al., 2004a). Moreover, a near-infrared analysis of a HMPO found collimated outflows with properties appearing to be scaled-up versions of low-mass outflows (Davis et al., 2004). This latter group

of observations favors an accretion scenario for the formation of massive stars that is a scaled up version of the low-mass scenario.

For both well-collimated and poorly collimated outflows, relations between outflow and source parameters hold over many orders of magnitude (e.g., Richer et al., 2000, Beuther et al., 2002c, Wu et al., 2004). Richer et al. point out that these correlations do not necessarily argue for a common entrainment or driving mechanism for sources of all luminosities given that one would expect that most physically reasonable outflow mechanisms would generate more powerful winds if the source mass and luminosity are increased. It is interesting to note that no well-collimated outflows have been observed toward a (proto)-O star (e.g., Shepherd, 2003, and references therein, Sollins et al., 2004). Thus, the link between accretion and outflow is not as well established for forming O stars as for early B stars and formation by coalescence may still be a possibility. Table 1 presents a number of relevant references for observations which shed light on massive outflows.

The current situation is that different observations find results which appear to contradict each other. In order to resolve this conflict, it is necessary to reevaluate the observations. In principle, three possibilities exist to solve the discrepancies: (a) some observations are wrongly interpreted, (b) there exist physically different modes of massive molecular outflows and thus massive star formation, or (c) the observed sources are not directly comparable, e.g., there might be evolutionary differences between the observed sources which could translate into various evolutionary signatures of the massive outflows.

It is possible that (a) applies to some of the single-dish results, e.g., the initial claim of low collimation for massive molecular outflows can be misinterpreted by the low spatial resolution of the observation, the generally larger distances to the sources and uncertainties due to the unknown inclination angles of the outflows. However, the results based on high-spatial-resolution observations are more significant and cannot be discarded in this manner. It appears that physically different modes and/or evolutionary differences must exist to explain all the observations. While we cannot exclude the possibility that different modes of star formation and their associated outflows exist, it seems unlikely given the link between accretion and outflow that has been established up to early B spectral types. Thus, here we propose an evolutionary scenario for massive outflows which is capable of explaining the morphological and energetic results within a consistent picture of massive protostellar evolution. This evolutionary scenario is based on the idea that stars of all masses form via similar accretion-based processes that are proposed for low-mass star formation (e.g., McKee and Tan, 2003).

Table 1. Summary of outflow results. This table does not claim completeness but gives an overview of relevant publications connected to the question of outflow evolution.

Source	Results	Ref
Low-spatial resolution single-dish studies		
122 UCHIIs	ubiquitous phenomena	1
10 UCHIIs	50% bipolarity, low collimation, \dot{M} vs L_{bol} relation	2
3 YSOs	\dot{M} vs L_{bol} still holds	3
11 YSOs	low collimation, no Hubble law, \dot{M} vs L_{bol} not correlated	4
69 HMPOs	55% bipolarity, accretion-outflow process suggested	5
26 HMPOs	80% bipolarity, no \dot{M} vs L_{bol} but M_{out} vs M_{core} , consistent with collimated outflows, similar to low-mass outflows	6
139, all types	M_{out} & \dot{M} correlate with L_{bol} , on average less collimated	7, 8
High-spatial resolution interferometer and infrared studies		
G192.16, HCHII	wide-angle wind + molecular flow & disk	9,10,11
IRAS20126, HCHII	precessing jet with disk	12,13
IRAS05358, HMPO	consistent with low-mass jets	14
W75N, HC/UCHII	energetics different to low-mass, not scaled up outflows	15
IRAS19410, HMPO	consistent with low-mass outflows	16
G35.2, HCHII	a cluster of collimated outflows	17
2 HMPOs	accretion based outflows	18
4 HMPOs/HCHIIs	same physical driving mechanisms as low-mass outflows	19
IRAS16547, HMPO	collimated jet, similar to low-mass jets	20,21
IRAS18151, HMPO	scaled-up versions of low-mass jets driven by disk accretion	22
G5.89, UCHII	multiple wide-angle outflows, harbors O5 star	23

The listed results just refer to mm studies of thermal lines and infrared studies. Ref: (1) Shepherd and Churchwell, 1996b, (2) Shepherd and Churchwell, 1996a, (3) Henning et al., 2000, (4) Ridge and Moore, 2001, (5) Zhang et al., 2001, (6) Beuther et al., 2002c, (7) Wu et al., 2004, (8) Wu et al., 2005, (9) Shepherd et al., 1998, (10) Devine et al., 1999, (11) Shepherd et al., 2001, (12) Cesaroni et al., 1999, (13) Shepherd et al., 2000, (14) Beuther et al., 2002a, (15) Shepherd et al., 2003, (16) Beuther et al., 2003, (17) Gibb et al., 2003, (18) Su et al., 2004, (19) Beuther et al., 2004a, (20) Garay et al., 2003, (21) Brooks et al., 2003, (22) Davis et al., 2004, (23) Sollins et al., 2004

2.2 A potential evolutionary scenario

Reevaluation of the high-spatial resolution literature presented in Table 1 shows that most of the youngest early B protostars (HMPOs and those producing hypercompact HII regions) support the idea that these high-mass outflows are driven by similar physical processes as those seen in low-mass outflows. Contrary to this, three sources in particular show different observational characteristics: G5.89: which harbors an O5 star and multiple wide-angle outflows, and G192.16 and W75N: two early B stars with UCHII regions. G192.16 and W75N VLA2 both appear to be relatively old (a few $\times 10^5$ years based on the CO dynamical timescale), and they have had adequate time to reach the main sequence and produce significant ionizing radiation. The outflows are poorly collimated within 100 AU of the central star and their outflow morphology on larger scales are consistent with wind-blown bubbles. Furthermore, it should

be noted that the single-dish outflow studies, which report a lower degree of collimation for massive outflows preferentially observed sources with UCHII regions (Shepherd and Churchwell, 1996a, Ridge and Moore, 2001). In contrast, most other single-dish surveys were directed toward samples of younger sources, namely HMPOs, observing higher collimation degrees consistent with low-mass outflows.

To date, the different observations have been interpreted either in favor of: (1) similar driving processes for outflows of all masses (e.g., Beuther et al., 2002c, Davis et al., 2004); or (2) that massive stars form via different physical processes like explosive coalescence or that the outflows are powered by a combination of accretion and deflected outflow. (e.g., Churchwell, 1999, Bally, 2002). Here, we propose a different, less controversial interpretation of the data: an evolutionary sequence for massive protostars. We consider two possible evolutionary sequences which could result in similar observable outflow signatures as shown in Figure 4.

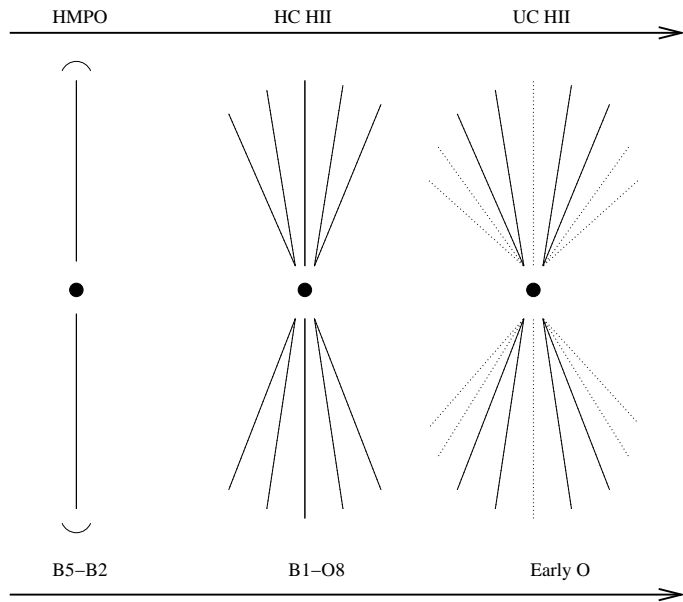


Figure 4. Sketch of the proposed evolutionary outflow scenario. The three outflow morphologies can be caused by two evolutionary sequences: (top) the evolution of an early B-type star from an HMPO via a HCHII region to an UCHII region, and (bottom) the evolution of an early O-type star which goes through B- and late O-type stages (only approximate labels) before reaching its final mass and stellar luminosity.

(a) The outflow evolution of an early B-type star: In the accretion scenario, a B star forms via accretion through a disk. During its earliest HMPO phase no HCHII region has formed yet, and the disk outflow interaction produces collimated jet-like outflows (Fig. 4 (left), e.g., IRAS05358). At some point, a

HCHII forms and the wind from the central massive star produces an additional less collimated outflow component. At that stage the disk is not entirely destroyed yet, and jet and wind can co-exist (Fig. 4 (center), e.g., IRAS 20126). Evolving further, a typical ultracompact HII region forms above and below the accretion disk and the massive wind begins to dominate the whole system (Fig. 4 (right), e.g., W75N). Remnants of the initial jet might still exist, and density gradients within the maternal core are likely to maintain at least a small degree of collimation at that stage.

(b) The outflow evolution of an early O-type star: An intriguing aspect of the outflow studies is that so far extremely collimated jet-like outflows have not been observed toward sources earlier than B1. It is possible that this is simply a selection effect because the evolutionary timescale of early O stars is expected to be only around 10^5 years (McKee and Tan, 2002). Given the scarcity of O stars and the short formation time, it is difficult to find sources while they are still in the earliest stages of formation. However, to form massive stars via accretion, the protostellar objects must accrete even after the central object has reached the main sequence. In this scenario, at the beginning, the massive protostar reaches a mid-B protostar-like state where it drives collimated outflows (Fig. 4 (left)). As the object continues to accrete it becomes an early-B to late-O star, forming a HCHII region while the wind and jet components could co-exist (Fig. 4 (center)). Finally, as the central star evolves, it may eventually become a mid- to early-O star. The increased radiation from the central star would generate significant Lyman- α photons and ionize the molecular outflowing gas even at large radii. The result may be an increase in the plasma pressure at the base of the outflow which could overwhelm the collimating effects of a magnetic field (e.g., Shepherd, 2003, Konigl and Pudritz, 2000). Incorporating the additional physical effects of high-mass protostars on the surrounding disk and envelope is one of the challenges of theoretical massive outflow modeling (e.g., Konigl, 1999). In this scenario, it would be intrinsically impossible to ever observe collimated jet-like outflows from very young early O-type (proto)stars.

2.3 Discussion and potential caveats

This scenario is not the only possible interpretation, and different physical processes could take place at the earliest stages of massive star formation. This reevaluation is based only on imaging data of thermal lines in the mm and infrared bands. However, many studies of outflows have also been undertaken by the means of maser studies, especially H₂O maser. While some maser studies found H₂O maser emission consistent with jet-like outflows (e.g. Kylafis and Pavlakis, 1999), other studies find shell-like expanding features which cannot be explained by collimated jets (e.g., Patel et al., 2000, Torrelles et al.,

2001, Torrelles et al., 2003). The most intriguing case is the H₂O maser study in W75N: Torrelles et al. (2003) find on projected spatial scales of 1400 AU that the two cm continuum sources VLA1 and VLA2 drive very different types of outflows, the first one appears to be a collimated jet whereas the second one rather resembles a wind-like shell. As the two sources are part of the same core, environmental properties cannot explain the difference. Both sources appear to have a similar luminosity (B1-B2 spectral types) although the spectral type derived for VLA1 should be considered an upper limit due to likely strong contamination by ionizing flux produced by shock waves in the jet (Shepherd et al., 2004). Assuming the VLA1 jet is produced by an early B star, then the difference in morphology would not be a question of the mass of the central source as well. Thus, Torrelles et al. (2003) propose that an evolutionary explanation is most likely. They cannot determine which source is younger but based on the extent of the maser emission – the non-collimated features are more compact – they suggest that the collimated jet might belong to the more evolved source. This would be a counter-example to the scenario presented in this paper as well as to the scenarios discussed for low-mass outflows (e.g., Andre et al., 2000). However, maser emission appears to be very selective, and many known outflow sources have no H₂O maser emission at all (e.g., Beuther et al., 2002c). Therefore, it is also possible that the collimated part of the outflow from VLA2 is simply not depicted by the data, and the non-collimated features have been excited more recently by the central HCHII region. Furthermore, the cm continuum emission from VLA1 may be due primarily to the jet (Shepherd et al., 2004). Thus, it is feasible that the central source of VLA1 is either less massive than VLA2 or it is younger and has not formed a HCHII region yet. Therefore, we might only observe a collimated feature toward this source. The latter scenario is consistent with the evolutionary sequence presented here. To properly differentiate between both scenarios in this source requires that we find other means to determine the age of the powering sources VLA1 and VLA2.

It should be stressed that the proposed evolutionary scenario is still only a potential, qualitative explanation for the observed outflow features which must be tested against both theory and observations.

References

Andre, P., Ward-Thompson, D., and Barsony, M. (2000). *Protostars and Planets IV*, pages 59.

Bachiller, R. and Tafalla, M. (1999). In *NATO ASIC Proc. 540: The Origin of Stars and Planetary Systems*, pages 227.

Bally, J. (2002). In *Hot Star Workshop III: The Earliest Stages of Massive Star Birth. ASP Conference Proceedings*, Vol. 267. Edited by Paul A. Crowther, pages 219.

Beckwith, S. V. W., Henning, T., and Nakagawa, Y. (2000). *Protostars and Planets IV*, pages 533.

Beuther, H. (2004). *in: X-Ray and Radio Connections*, *astro-ph/0404563*.

Beuther, H. and Schilke, P. (2004). *Science*, 303:1167–1169.

Beuther, H., Schilke, P., and Gueth, F. (2004a). *ApJ*, 608:330–340.

Beuther, H., Schilke, P., Gueth, F., et al. (2002a). *A&A*, 387:931–943.

Beuther, H., Schilke, P., Menten, K. M., et al., (2002b). *ApJ*, 566:945–965.

Beuther, H., Schilke, P., Sridharan, T. K., et al., (2002c). *A&A*, 383:892–904.

Beuther, H., Schilke, P., and Stanke, T. (2003). *A&A*, 408:601–610.

Beuther, H., Walsh, A., Schilke, P., et al., (2002d). *A&A*, 390:289–298.

Beuther, H., Zhang, Q., Greenhill, L. J., et al., (2004b). *ApJ*, 616:L31–L34.

Blake, G. A., Sutton, E. C., Masson, C. R., and Phillips, T. G. (1987) *ApJ*, 315:621.

Bonnell, I. A., Bate, M. R., and Zinnecker, H. (1998). *MNRAS*, 298:93–102.

Bonnell, I. A., Vine, S. G., and Bate, M. R. (2004). *MNRAS*, 349:735–741.

Brooks, K. J., Garay, G., Mardones, D., and Bronfman, L. (2003). *ApJ*, 594:L131–L134.

Cesaroni, R., Felli, M., Jenness, T., Neri, R., Olmi, L., Robberto, M., Testi, L., Walmsley, C. M. (1999) *A&A*, 345:949–964.

Cesaroni, R. (2004). *in: Astrophysics and Space Science*, *in press*.

Churchwell, E. (1999). In *NATO ASIC Proc. 540: The Origin of Stars and Planetary Systems*, pages 515.

Churchwell, E. (2002). *ARA&A*, 40:27–62.

Codella, C., Lorenzani, A., Gallego, A. T., Cesaroni, R., and Moscadelli, L. (2004). *A&A*, 417:615–624.

Davis, C. J., Varricatt, W. P., Todd, S. P., and Ramsay Howat, S. K. (2004). *A&A*, 425:981–995.

Devine, D., Bally, J., Reipurth, B., et al., (1999). *AJ*, 117:2919–2930.

Egan, M. P., Shipman, R. F., Price, S. D., et al., (1998). *ApJ*, 494:L199+.

Evans, N. J., Shirley, Y. L., Mueller, K. E., and Knez, C. (2002). In *Hot Star Workshop III: The Earliest Stages of Massive Star Birth. ASP Conference Proceedings*, Vol. 267. Edited by Paul A. Crowther, pages 17.

Garay, G., Brooks, K. J., Mardones, D., and Norris, R. P. (2003). *ApJ*, 587:739–747.

Garay, G., Faundez, S., Mardones, D., et al., (2004). *ApJ*, 610:313–319.

Garay, G. and Lizano, S. (1999). *PASP*, 111:1049–1087.

Gibb, A. G., Hoare, M. G., Little, L. T., and Wright, M. C. H. (2003). *MNRAS*, 339:1011–1024.

Henning, T., Schreyer, K., Launhardt, R., and Burkert, A. (2000). *A&A*, 353:211–226.

Hogerheijde, M. R. and Sandell, G. (2000). *ApJ*, 534:880–893.

Hunter, T. R. (1997). *Ph.D. Thesis*.

Jijina, J. and Adams, F. C. (1996). *ApJ*, 462:874.

Keto, E. (2003). *ApJ*, 599:1196–1206.

Konigl, A. (1999). *New Astronomy Reviews*, 43: 67–77.

Konigl, A. and Pudritz, R. E. (2000). *Protostars and Planets IV*, pages 759.

Kurtz, S., Cesaroni, R., Churchwell, E., et al., (2000). *Protostars and Planets IV*, pages 299.

Kurtz, S., Churchwell, E., and Wood, D. O. S. (1994). *ApJS*, 91:659–712.

Kylafis, N. D. and Pavlakis, K. G. (1999). In *NATO ASIC Proc. 540: The Origin of Stars and Planetary Systems*, pages 553.

McKee, C. F. and Tan, J. C. (2002). *Nature*, 416:59–61.

McKee, C. F. and Tan, J. C. (2003). *ApJ*, 585:850–871.

Minier, V., Booth, R. S., and Conway, J. E. (2000). *A&A*, 362:1093–1108.

Molinari, S., Brand, J., Cesaroni, R., and Palla, F. (1996). *A&A*, 308:573–587.

Molinari, S., Brand, J., Cesaroni, R., and Palla, F. (2000). *A&A*, 355:617–628.

Motte, F., Andre, P., and Neri, R. (1998). *A&A*, 336:150–172.

Mueller, K. E., Shirley, Y. L., Evans, N. J., and Jacobson, H. R. (2002). *ApJS*, 143:469–497.

Norberg, P. and Maeder, A. (2000). *A&A*, 359:1025–1034.

Norris, R. P., Byleveld, S. E., Diamond, P. J., et al., (1998). *ApJ*, 508:275–285.

Ossenkopf, V. and Henning, T. (1994). *A&A*, 291:943–959.

Patel, N. A., Greenhill, L. J., Herrnstein, J., et al., (2000). *ApJ*, 538:268–274.

Pestalozzi, M. R., Elitzur, M., Conway, J. E., and Booth, R. S. (2004). *ApJ*, 603:L113–L116.

Richer, J. S., Shepherd, D. S., Cabrit, S., Bachiller, R., and Churchwell, E. (2000). *Protostars and Planets IV*, pages 867.

Ridge, N. A. and Moore, T. J. T. (2001). *A&A*, 378:495–508.

Salpeter, E. E. (1955). *ApJ*, 121:161.

Scalo, J. (1998). In *ASP Conf. Ser. 142: The Stellar Initial Mass Function (38th Herstmonceux Conf.)*, pages 201.

Schilke, P., Groesbeck, T. D., Blake, G. A., and Phillips, T. G. (1997). *ApJS*, 108:301.

Shepherd, D. S. and Churchwell, E. (1996a). *ApJ*, 472:225.

Shepherd, D. S. and Churchwell, E. (1996b). *ApJ*, 457:267.

Shepherd, D. S., Watson, A. M., Sargent, A. I., and Churchwell, E. (1998). *ApJ*, 507:861–873.

Shepherd, D. S., Yu, K. C., Bally, J., and Testi, L. (2000). *ApJ*, 535:833.

Shepherd, D. S., Claussen, M. J., & Kurtz, S. E. (2001). *Science*, 292:1513–1518.

Shepherd, D. (2003). In *ASP Conf. Ser. 287: Galactic Star Formation Across the Stellar Mass Spectrum*, pages 333–344.

Shepherd, D. S., Testi, L., and Stark, D. P. (2003). *ApJ*, 584:882–894.

Shepherd, D. S., Kurtz, S. E., and Testi, L. (2004). *ApJ*, 601:952–961.

Shirley, Y. L., Evans, N. J., Young, K. E., et al., (2003). *ApJS*, 149:375–403.

Shu, F. H., Najita, J. R., Shang, H., and Li, Z.-Y. (2000). *Protostars and Planets IV*, pages 789.

Sollins, P. K., Hunter, T. R., Battat, J., et al., (2004). *ApJ*, 616:L35–L38.

Sridharan, T. K., Beuther, H., Schilke, P., et al., (2002). *ApJ*, 566:931–944.

Stahler, S. W., Palla, F., and Ho, P. T. P. (2000). *Protostars and Planets IV*, pages 327.

Su, Y., Zhang, Q., and Lim, J. (2004). *ApJ*, 604:258–271.

Torrelles, J. M., Gomez, J. F., Rodriguez, L. F., et al., (1998). *ApJ*, 505:756–765.

Torrelles, J. M., Patel, N. A., Anglada, G., et al., (2003). *ApJ*, 598:L115–L119.

Torrelles, J. M., Patel, N. A., Gomez, J. F., et al., (2001). *Nature*, 411:277–280.

Walmsley, M. (1995). In *Revista Mexicana de Astronomia y Astrofisica Conference Series*, pages 137.

Walsh, A. J., Burton, M. G., Hyland, A. R., and Robinson, G. (1998). *MNRAS*, 301:640–698.

Williams, S. J., Fuller, G. A., and Sridharan, T. K. (2004). *A&A*, 417:115–133.

Wilson, T. L., Gaume, R. A., Gensheimer, P., and Johnston, K. J. (2000). *ApJ*, 538:665–674.

Wood, D. O. S. and Churchwell, E. (1989). *ApJ*, 340:265–272.

Wu, Y., Wei, Y., Zhao, M., et al., (2004). *A&A*, 426:503–515.

Wu, Y., Zhagn, Q., Chen, H., et al., (2005). *ApJ in press*.

Yorke, H. W. and Sonnhalter, C. (2002). *ApJ*, 569:846–862.

Zhang, Q., Hunter, T. R., Brand, J., et al., (2001). *ApJ*, 552:L167–L170.

This figure "beuther_fig1a.gif" is available in "gif" format from:

<http://arxiv.org/ps/astro-ph/0502214v1>

This figure "beuther_fig1b.gif" is available in "gif" format from:

<http://arxiv.org/ps/astro-ph/0502214v1>

This figure "beuther_fig1c.gif" is available in "gif" format from:

<http://arxiv.org/ps/astro-ph/0502214v1>

This figure "beuther_fig2.gif" is available in "gif" format from:

<http://arxiv.org/ps/astro-ph/0502214v1>